A Stepwise Design and Implementation of a Fan Speed PID Controller Using Discrete Analog Components

Marawan Abdulsattar

Abstract

This project presents the design, simulation, and physical implementation of an analog PID (Proportional–Integral–Derivative) controller for regulating the speed of a 12V DC fan using only discrete, analog components. The development followed a staged approach: initial prototyping and control were performed using a microcontroller to build foundational understanding and tune control parameters using the Ziegler–Nichols method. Subsequently, the system was transitioned to an analog circuit, simulated in Multisim to model the PID and feedback behavior. Finally, the complete circuit was constructed and physically tuned. The implementation addressed several practical challenges, including unstable feedback signals, frequency-to-voltage conversion, dual-supply requirements for op-amps, and the absence of feedback at low setpoints. A hardware-based kick-start mechanism was introduced to overcome the latter issue. The final analog controller demonstrated stable speed regulation and robustness to disturbances, highlighting the viability of analog PID design in educational and low-cost control applications.

https://github.com/Marawan29/PIDControllerProject

1. Introduction

PID (Proportional–Integral–Derivative) controllers are fundamental building blocks in control systems engineering, widely applied in industrial, automotive, and consumer electronics for precise regulation of physical processes. While the mathematical foundation of PID control is well established, practical implementation—particularly in analog circuitry—remains a valuable yet challenging exercise for engineering students.

This project was conducted as part of a university course assignment requiring the design and construction of a fully analog PID controller using only discrete components, with no digital or programmable devices. The target application selected by the team was a **fan speed control system**, a classic control problem involving a nonlinear electromechanical plant and frequency-based feedback.

Given the inherent difficulty of designing analog control systems from scratch, the team adopted a structured, phased methodology to reduce complexity and build a solid understanding of system behavior before hardware implementation. The approach consisted of three main stages:

1. **Digital Prototyping:**
   A microcontroller-based control system was first developed to read the fan's tachometer signal, generate control output, tune the PID parameters using the Ziegler–Nichols method, and approximating the transfer function of the system. This phase allowed rapid iteration and intuitive understanding of system dynamics.

2. **Simulation and Analog Design:**
   The PID controller was then translated into an analog design and simulated using Multisim 14.3. Textbook methods were consulted to compute component values, and a frequency-to-voltage converter was incorporated to emulate the fan's tachometer feedback in analog form.

3. **Physical Implementation:**
   The final stage involved building the circuit on hardware, tuning it with potentiometers, and resolving practical challenges such as op-amp supply requirements and edge cases where feedback became unavailable. A custom kick-start mechanism was implemented to overcome startup deadlock when the setpoint was zero.

Throughout the project, the team encountered and overcame a variety of real-world design constraints, including feedback instability, voltage amplification, and dual-rail power supply issues. By combining

theoretical analysis, simulation, and hands-on troubleshooting, the project provided a comprehensive learning experience in analog control systems.

2. System Overview

The implemented system is a closed-loop analog control circuit designed to regulate the speed of a 12V DC brushless fan using a PID control strategy. The system consists of the following major functional blocks:

- **Plant (Fan):** A standard three-wire brushless DC fan, with red and black wires for power and a yellow wire for tachometer feedback. The fan's speed is intrinsically controlled by its input voltage, while its rotational speed is encoded in the frequency of the tachometer signal, which pulls low twice per revolution.

- **Setpoint Input:** A variable voltage source representing the desired fan speed. This is compared to the measured feedback to generate the control error signal.

- **Feedback Signal Transducer:**
  Since the fan outputs a frequency-based tachometer signal, a *frequency-to-voltage (F–V) conversion* stage is required to generate a proportional voltage signal for feedback. This stage is built using an LM2907N F–V converter IC, which converts the digital pulse signal from the fan into a continuous voltage corresponding to its RPM.

- **Instrumentation Difference Amplifier:**
  An Instrumentation Difference Amplifier is used to generate the error signal and provide a high input impedance to not load the feedback signal or the setpoint.

- **Analog PID Controller:**
  The core of the system is a fully analog PID controller constructed using op-amps and discrete components. The control algorithm is implemented by designing the standard PID transfer function in analog circuitry:

$$U(s) = K_p E(s) + K_i \frac{1}{s} E(s) + K_d s E(s)$$

  where $E(s)$ is the error between the setpoint and the measured fan speed. Each term is implemented using integrator, differentiator, and gain amplifier circuits based on resistor-capacitor networks and operational amplifiers.

- **Output Driver Stage:**
  The output of the analog PID controller is a control voltage that modulates the fan's power. However, the fan requires more current and voltage than typical op-amps can provide. Thus, a power amplification stage is added using a TIP122 Darlington transistor in a low-side or emitter-follower configuration, depending on the design phase. This ensures the fan receives sufficient drive current while remaining under the control of the PID voltage output.

- **Power Supply System:**
  Due to the requirements of the op-amp circuits, the system requires a symmetric ± 24V power supply. Several approaches were investigated (including virtual ground circuits and DC-DC conversion), but ultimately dual isolated supplies were used to ensure stability and sufficient headroom for the analog stages.

3. Methodology

To successfully design and implement a fully analog PID controller for fan speed regulation, a structured, three-phase methodology was adopted. Each phase served a distinct purpose in developing a robust understanding of the system dynamics, validating control strategies, and resolving practical limitations prior to final hardware implementation.

3.1. Phase I – Digital Prototyping and Validation

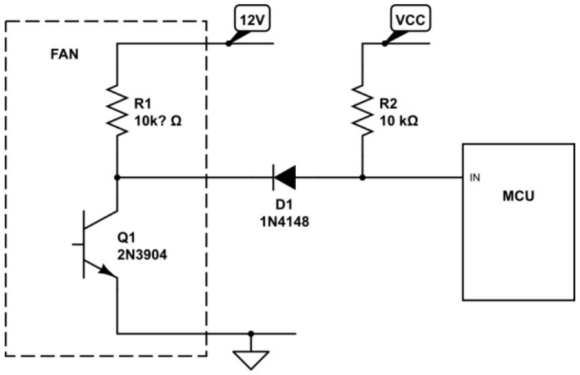

Figure 1. Pull up resistor network connected to the MCU.

The project began with a microcontroller-based prototype to validate the control concept and characterize the fan behavior. The objective was to emulate a closed-loop control system using digital tools, allowing rapid testing and parameter tuning.

A 12V three-wire brushless DC fan was selected as the plant, Appendix A Figure [11]. The yellow wire provided a tachometer output signal which toggles low twice per revolution. Initial attempts to read this signal on the microcontroller required the integration of a pull-up resistor network, and further improvements were made by isolating the feedback signal using a diode to enhance stability as in Figure [1], particularly at voltages below 12V.

Fan actuation was achieved using a TIP122 Darlington transistor configured in a common-drain topology as an output stage. Since the microcontroller could only output a 3.3V PWM signal, this was first passed through an RC lowpass filter to obtain a proportional analog voltage and then amplified to 12V using an opamp stage. The circuit schematic is shown in Figure [2].

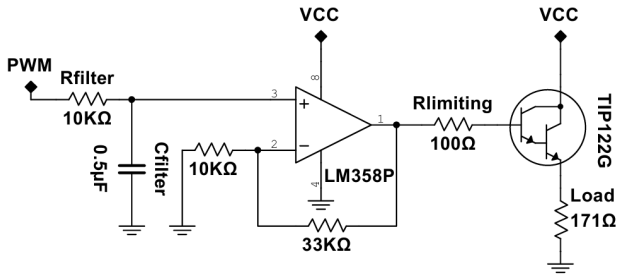

Figure 2. Output-stage and PWM transducer.

The time constant for the filter is

$$\tau = R \cdot C = 10\,\mathrm{k\Omega} \cdot 0.5\,\mu\mathrm{F} = 5\,\mathrm{ms}$$

And as the system reaches the desired response after about 5τ, the control action should be taken at most 1 time per $25ms$, but we take it once per $100ms$.

A discrete PID control algorithm was then implemented in code, included in Appendix C, then parameters were tuned using the Ziegler–Nichols method. This allowed the team to determine a set of gain values that provided satisfactory performance, which later served as a baseline for the analog implementation.

Also, a series of step inputs were applied and sensor data was recorded, to obtain a transfer function approximation for the plant using those data and the Matlab system identification toolbox. The system was also simulated and tuned using Simulink as a second step verification for the results obtained using the Ziegler-Nichols method.

3.2. Phase II – Simulation and Analog Design

With verified control parameters and working knowledge of the system dynamics, the team transitioned to the analog domain. Multisim 14.3 was chosen for its robust component libraries and ease of use as a virtual laboratory environment.

The analog PID controller was constructed using opamps, resistors, and capacitors. Various textbooks were consulted for multiple circuit topologies and design recommendations. The schematic is divided into four main stages, instrumentation differential amplifier as shown in Figure [3], controller as in Figure [6] and output stage similar to the one used with the micro-controller. The final simulation modeled the fan load using the transfer function obtained using system identification toolbox.

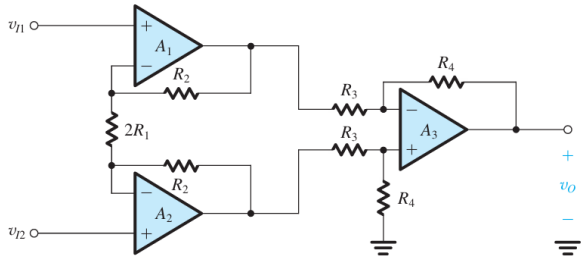

Figure 3. High-input-resistance difference amplifier / Instrumentation Amplifier. $v_O = \frac{R_4}{R_3}\left(1 + \frac{R_2}{R_1}\right) v_{Id}$

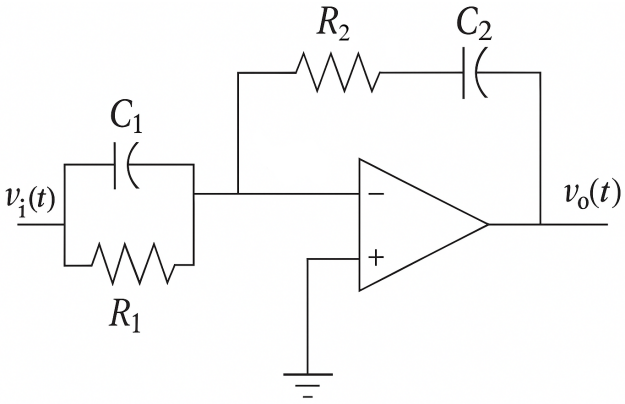

Figure 4. Second-order opamp implementing the three PID operations. $H(s) = -\left[\left(\frac{R_2}{R_1} + \frac{C_1}{C_2}\right) + R_2 C_1 s + \frac{1}{R_1 C_2 s}\right]$

The final schematic with the values chosen for the various components is shown in Figure [4], with some practical design considerations, such as bias currents

of op-amps, filtering the differential controller output to eliminate kickstart and high-frequency amplification, and reset switch for the integral-windup scenarios, etc. The logic behind the chosen values is to achieve specific gain requirements and practical considerations. All gains values are easily understood considering what we have discussed so far.

Since the fan's feedback was frequency-based, a critical component was the design of a frequency-to-voltage (F–V) converter transducer. After evaluating several discrete solutions, the LM2907N F–V converter IC was selected for its reliability and practicality. Extensive effort was required to obtain a working SPICE model and to correctly simulate the chip's behavior using data sheet specifications and trial-and-error adjustments, see Appendix A for more details about this chip and equations of V_out and V_ripple. Final schematic with components values is shown in Figure [6]. This part was designed in an agile approach, with iterations between physical implementation and simulation. Although simulated results were initially inconsistent, these discrepancies were attributed to the differences between signal generation in Multisim and real-world tach behavior.

3.3. Phase III – Hardware Implementation and Testing

In the final phase, the circuit was implemented physically using breadboards and discrete components. The lessons learned from simulation significantly reduced the number of design iterations needed.

Power supply design emerged as a major consideration. The analog circuit required dual rails (V) to accommodate the op-amps output swing. Initial strategies such as voltage dividers and boost converters proved inefficient or unstable. Ultimately, two dedicated 12V supplies were used to ensure consistent operation. Also the control action required more than 12V to acheive the required time response, hence why we splitted our supply as +18V for the postive rail and -6V for negative rail, and amplified the PID output thrice in the postive rail which is the control action which is mainly postive. This resulted in the PID reducuing the range of the PID controller output, and benfiting of that range in the control action.

Although the PID controller circuit simulated was physically test and proved working, a separate op-amp for each controller and compensator was used as shown in Figure [7] to decouple the transfer functions and make tuning the controller easier.

The full circuit was assembled and tuned using potentiometers to adjust gain values in each PID path. Real-time tuning was essential to accommodate component tolerances, measurement errors, and nonlinearities in the system response.

A significant issue occurred when the setpoint reached zero RPM: the feedback signal ceased, and the setpoint is replicated on the other terminal of the differential pair. producing zero error and preventing the loop from reactivating. To overcome this deadlock, a manual "kick-start" button hot-fix was introduced to inject a temporary pulse into the F–V converter, emulating a feedback signal to restart the fan. Further investigations about why that happens were done and are discussed in the results section. Throughout testing, the system exhibited robust performance. Minor disturbances such as additional load resistances had negligible impact on fan speed, demonstrating effective disturbance rejection.

4. Experiments and Results

The development process of the analog PID controller spanned multiple implementation phases, each yielding critical insights into system behavior, stability, and real-world viability. This section presents the experimental observations, functional outcomes, and performance evaluation of the control system in both simulated and physical environments.

4.1. Digital Prototype Results

In the initial phase, the microcontroller-based prototype allowed rapid testing and parameter exploration. After resolving the initial instability in reading the tachometer signal—through the introduction of a pull-up resistor and a diode for signal isolation—the feedback system proved reliable. The microcontroller-driven PWM output was successfully filtered using an RC low-pass network, producing a clean analog voltage that drove the fan effectively via the TIP122 transistor stage. We where able to apply Ziegler-Nichols method and obtain the following ultimate gain and ultimate period of oscillation.

$$K_u = 4, \quad P_u = 400\,\text{ms}$$

The Ziegler–Nichols tuning method yielded a set of PID parameters that provided relatively fast settling time and minimal overshoot, laying the foundation for subsequent analog implementation. This stage confirmed both the feasibility of fan speed control and the behavioral characteristics of the plant, such as its nonlinear response at lower voltages.

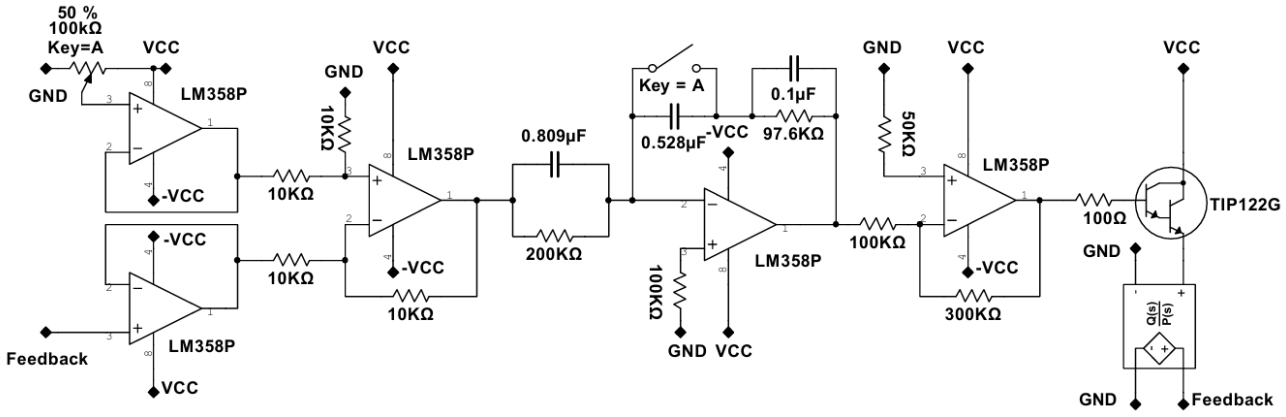

Figure 5. Final controller schematic.

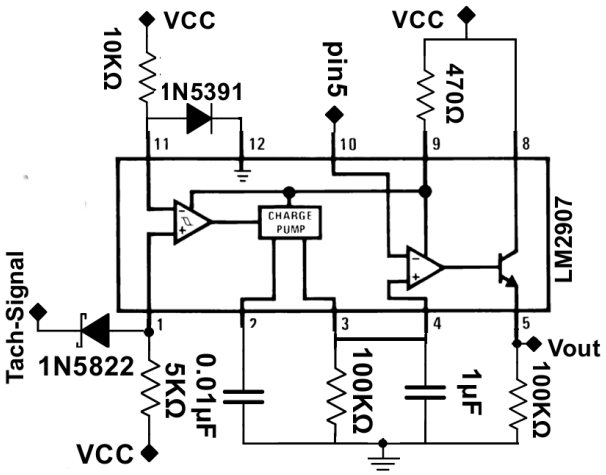

Figure 6. F-to-V converter feedback transducer.

We also proceeded with system identification in order to obtain system transfer function. Applying a series of step inputs and recording the system output is shown in Figure [8]

System Identification Toolbox was then used to obtain a transfer function approximation for the system, the fit to the data was 70%. The transfer function is

$$\frac{49.75}{s^2 + 17.27s + 49.34}$$

We then used Simulink to simulate the system and tune the PID controller parameters.

$$C(s) = K_p + \frac{K_i}{s} + \frac{K_d N}{s+N} = 2.09 + \frac{9.2}{s} + \frac{0.079 \cdot 2}{1 + \frac{2}{s}}$$

The Simulink step response is shown in Figure [9]

4.2. Simulation Results

The analog circuit was tested using Multisim 14.3, incorporating all designed components including the PID controller and frequency-to-voltage converter. The step response of the simulated circuit is shown in Figure [10]. The system response is Almost Identical to the Simulink simulation, which indicates that the circuit is working as intended, with the same following transient characteristics.

$\%OS = 10\%, \quad T_r = 200\,\text{ms}, \quad T_p = 400\,\text{ms}, \quad T_s = 750\,\text{ms}$

Some discrepancies between expected and simulated behavior—particularly with the LM2907N frequency-to-voltage converter—were identified and traced back to signal conditioning and model limitations. These were largely anticipated and confirmed during physical implementation, validating the simulation's utility as an intermediate validation step.

Tuning of the gain stages in simulation helped predict the necessary component ranges and guided practical component selection.

4.3. Hardware Results

The final hardware implementation reflected most of the behavior observed in simulation, albeit with expected deviations due to real-world factors such as component tolerances, supply noise, and nonlinear-

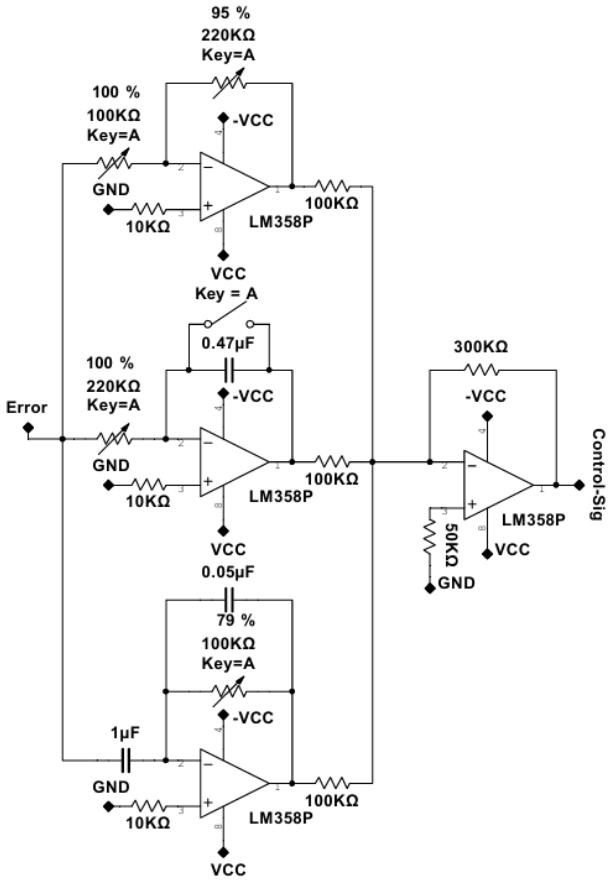

Figure 7. Actual PID controller circuit used.

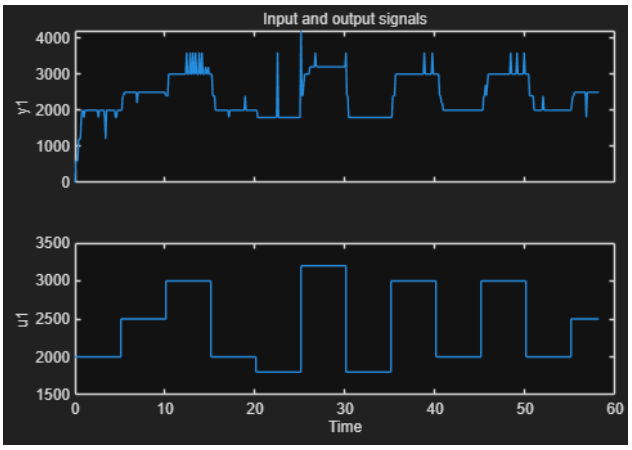

Figure 8. Input series of step functions and system output.

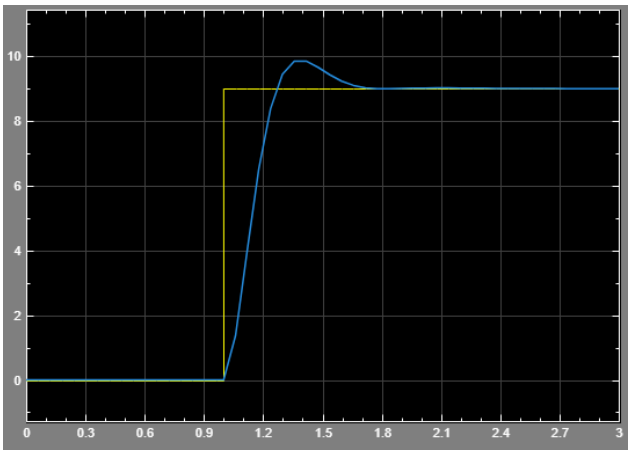

Figure 9. Step response of the system Simulink simulation.

ities. After sourcing dual ±24 V power supplies to properly bias the op-amps, the analog PID controller operated effectively.

Manual tuning via potentiometers was used to refine the system's responsiveness. The final configuration demonstrated stable fan speed regulation, robust disturbance rejection, and minimal steady-state error. The controller was capable of adapting to variations in setpoint voltage without significant overshoot or oscillation.

A notable practical issue emerged when the setpoint voltage was zero: the absence of tachometer pulses resulted in no feedback signal, halting loop activity. This condition was resolved with a manual kick-start button that injects a mock feedback pulse to reinitialize the control loop. While this was not part of the original design, it highlights the importance of anticipating edge cases in control systems.

To further evaluate system robustness, resistive disturbances were introduced in series with the fan. The controller consistently compensated for the load variations, maintaining steady fan speed, which demonstrated the effectiveness of the PID controller in practical operating conditions.

5. Future Directions

While the current implementation achieved robust and functional analog control over fan speed using a PID architecture, several theoretical and practical extensions could significantly enhance the system's flexibility, efficiency, and real-world applicability. This section outlines potential avenues for future development.

5.1. Integration of Adaptive Control

The present system relies on fixed PID parameters determined through tuning and experimentation. How-

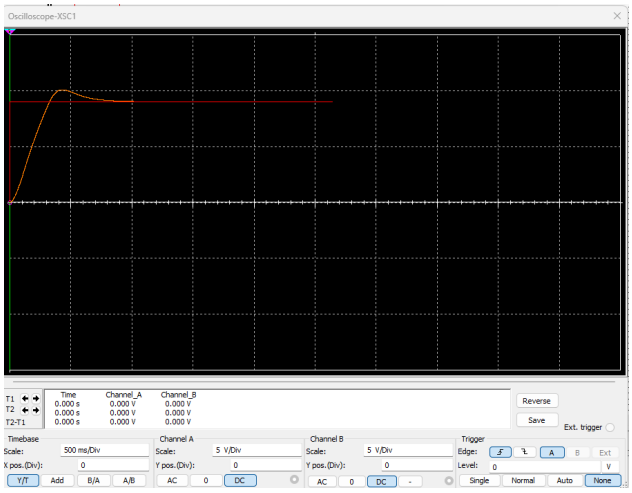

Figure 10. Step response of the system Multisim simulation.

ever, fan dynamics may vary with temperature, load conditions, or aging of components. An adaptive analog control scheme—possibly leveraging variable gain elements such as digitally controlled potentiometers or voltage-controlled amplifiers—could adjust controller parameters in real-time, maintaining optimal performance across varying operating conditions.

5.2. Replacement of Dual Supply Requirement

One of the key practical limitations was the necessity of a dual $\pm 24\,\mathrm{V}$ supply for op-amp biasing. Future designs may explore rail-to-rail op-amps powered by a single supply, coupled with signal conditioning strategies (e.g., DC bias shifting or pseudo-differential architectures). This would reduce power complexity and enhance the portability and integration potential of the controller.

5.3. Compact Feedback Transducer Design

The frequency-to-voltage converter (LM2907N) used for feedback introduces a bulky and sensitive stage in the circuit. Future versions may involve custom-designed frequency decoder circuits or phase-locked loop (PLL)-based feedback mechanisms that provide greater linearity, higher frequency resolution, and lower susceptibility to noise.

5.4. Digital Hybrid Implementation

Although the core requirement was to avoid digital control, a hybrid system may combine analog PID regulation with digital monitoring and diagnostics. This could be achieved using micro-controllers purely for system health logging, safety thresholds, and visualization, without interfering in the control loop directly—preserving the analog design ethos while adding modern usability.

5.5. Support for Multiple Actuators and Load Types

The current implementation targets a single fan. Future versions may generalize the control architecture to support multiple actuators or different types of electromechanical loads, such as DC motors or pumps. This would require modular signal stages and configurable loop parameters to maintain control integrity across devices.

6. Contributions

This project provides a practical case study in bridging the gap between ideal control theory and real-world analog implementation. By developing a PID-based fan speed control system using discrete components, it highlights key non-idealities—such as feedback signal behavior, power supply constraints, and op-amp limitations—and documents effective strategies to overcome them. The work also integrates microcontroller prototyping as a learning scaffold, aiding intuition before transitioning to physical circuitry. It serves as a valuable reference for hands-on analog control design in educational settings.

Acknowledgments

We would like to express our sincere gratitude to **Professor Nader Mansour** for his invaluable guidance, continuous support, and the flexibility he provided regarding project deadlines, which allowed us to deeply explore both theoretical and practical aspects of control systems.

We are also grateful to **Dr. Mohammed Anwar** for his generous assistance with laboratory equipment and instrumentation, which was essential to the successful implementation and testing of our hardware circuit.

Their support and encouragement were instrumental in the completion of this project.

References

Automation, C. Analog electronic pid controllers. https://control.com/textbook/closed-loop-control/analog-electronic-pid-controllers/, 2025. Accessed: 2025-06-19.

Instruments, T. Pid control of brushless dc motors us-

Figure 11. A 12V DC brush-less fan used as a plant

ing analog components. Technical Report SLAA088, Texas Instruments, 2007. URL https://www.ti.com/lit/an/snaa088/snaa088.pdf. Accessed: 2025-06-19.

Maetschke, S. Read fan speed signal with arduino. https://www.makerguides.com/how-to-read-fan-speed-signal-with-arduino/, 2024. Accessed: 2025-06-19.

Nise, N. S. *Control Systems Engineering*. Wiley, 7 edition, 2015. ISBN 9781118170519.

Sedra, A. S., Smith, K. C., Carusone, T. C., and Gaudet, V. *Microelectronic Circuits*. Oxford University Press, 8 edition, 2020. ISBN 9780190853464.

Vorpérian, V. *Fast Analytical Techniques for Electrical and Electronic Circuits*. Cambridge University Press, 2002. ISBN 9780521624428.

()

A. Extra Material

Figure [11]

B. HOW TO USE LM2907N

Basic f to V Converter

The operation of the LM2907, LM2917 series is best understood by observing the basic converter shown in **Figure 3**. In this configuration, a frequency signal is applied to the input of the charge pump at pin 1. The voltage appearing at pin 2 will swing between two values which are approximately $1/4\ (V_{CC}) - V_{BE}$ and $3/4\ (V_{CC}) - V_{BE}$. The voltage at pin 3 will have a value equal to $V_{CC} \cdot f_{IN} \cdot C1 \cdot R1 \cdot K$, where K is the gain constant (normally 1.0).

The emitter output (pin 4) is connected to the inverting input of the op amp so that pin 4 will follow pin 3 and provide a low impedance output voltage proportional to input frequency. The linearity of this voltage is typically better than 0.3% of full scale.

Choosing R1, C1 and C2

There are some limitations on the choice of R1, C1 and C2 (**Figure 3**) which should be considered for optimum performance. C1 also provides internal compensation for the charge pump and should be kept larger than 100 pF. Smaller values can cause an error current on R1, especially at low temperatures. Three considerations must be met when choosing R1.

First, the output current at pin 3 is internally fixed and therefore V3 max, divided by R1, must be less than or equal to this value.

$$R1 \geq \frac{V3_{max}}{I_{3MIN}}$$

where V3 max is the full scale output voltage required from the converter and I_{3MIN} is the output sink current (150 μA)

Second, if R1 is too large, it can become a significant fraction of the output impedance at pin 3 which degrades linearity. Finally, ripple voltage must be considered, and the size of C2 is affected by R1. An expression that describes the ripple content on pin 3 for a single R1, C2 combination is:

$$V_{RIPPLE} = \frac{V_{CC}}{2 \cdot C2} \cdot C1 \left(1 - \frac{V_{CC} \cdot f_{IN} \cdot C1}{I_p}\right)_{p\text{-}p}$$

It appears R1 can be chosen independent of ripple, however response time, or the time it takes Vout to stabilize at a new frequency increases as the size of C2 increases, so a compromise between ripple, response time, and linearity must be chosen carefully. R1 should be selected according to the following relationship:

C is selected according to:

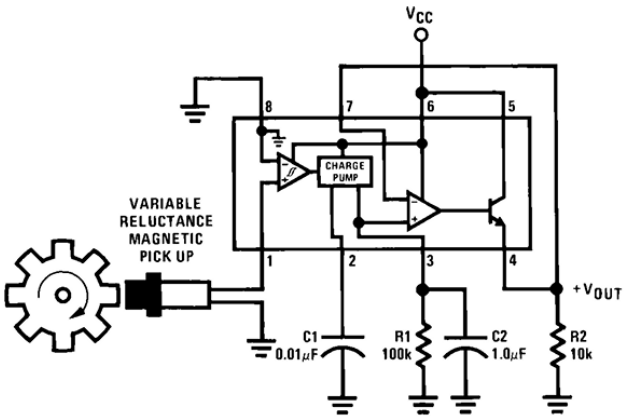

Figure 12. Basic F-to-V Converter

$$C1 = \frac{V3 \text{ Full Scale}}{R1 \cdot V_{CC} \cdot f_{\text{FULL SCALE}}}$$

Next decide on the maximum ripple which can be accepted and plug into the following equation to determine C2:

$$C2 = \frac{V_{CC}}{2 \cdot V_{\text{RIPPLE}}} \cdot C1 \left(1 - \frac{V3}{R1 \cdot I_2}\right)$$

The kind of capacitor used for timing capacitor C1 will determine the accuracy of the unit over the temperature range. **Figure 15** illustrates the tachometer output as a function of temperature for the two devices. Note that the LM2907 operating from a fixed external supply has a negative temperature coefficient which enables the device to be used with capacitors which have a positive temperature coefficient and thus obtain overall stability. In the case of the LM2917 the internal zener supply voltage has a positive coefficient which causes the overall tachometer output to have a very low temperature coefficient and requires that the capacitor temperature coefficient be balanced by the temperature coefficient of R1.

Using Zener Regulated Options (LM2917)

For those applications where an output voltage or current must be obtained independently of the supply voltage variations, the LM2917 is offered. The reference typically has an 11V source impedance. In choosing a dropping resistor from the unregulated supply to the zener note that the tachometer and op amp circuitry alone require about 3 mA at the zener voltage level provided by the zener. At low supply voltages,

C. Code

https://github.com/Marawan29/PIDControllerProject